

A Patient-Independent Neonatal Seizure Prediction Model Using Reduced Montage EEG and ECG

Sithmini Ranasingha^{1*}, Agasthi Haputhanthri¹, Hansa Marasinghe¹, *Member, IEEE*, Nima Wickramasinghe², Kithmin Wickremasinghe³, Jithangi Wanigasinghe⁴, Chamira U. S. Edussooriya¹ *Senior Member, IEEE*, and Joshua P. Kulasingham^{1†}, *Member, IEEE*

Abstract—Neonates are highly susceptible to seizures, often leading to short or long-term neurological impairments. However, clinical manifestations of neonatal seizures are subtle and often lead to misdiagnoses. This increases the risk of prolonged, untreated seizure activity and subsequent brain injury. Continuous video electroencephalogram (cEEG) monitoring is the gold standard for seizure detection. However, this is an expensive evaluation that requires expertise and time. In this study, we propose a convolutional neural network-based model for early prediction of neonatal seizures by distinguishing between interictal and preictal states of the EEG. Our model is patient-independent, enabling generalization across multiple subjects, and utilizes mel-frequency cepstral coefficient matrices extracted from multichannel EEG and electrocardiogram (ECG) signals as input features. Trained and validated on the Helsinki neonatal EEG dataset with 10-fold cross-validation, the proposed model achieved an average accuracy of 97.52%, sensitivity of 98.31%, specificity of 96.39%, and F1-score of 97.95%, enabling accurate seizure prediction up to 30 minutes before onset. The inclusion of ECG alongside EEG improved the F1-score by 1.42%, while the incorporation of an attention mechanism yielded an additional 0.5% improvement. To enhance transparency, we incorporated SHapley Additive exPlanations (SHAP) as an explainable artificial intelligence method to interpret the model and provided localization of seizure focus using scalp plots. The overall results demonstrate the model's potential for minimally supervised deployment in neonatal intensive care units, enabling timely and reliable prediction of neonatal seizures, while demonstrating strong generalization capability across unseen subjects through transfer learning.

Index Terms—attention, convolutional neural network (CNN), deep learning, electroencephalogram (EEG), electrocardiogram (ECG), explainability, mel-frequency cepstral coefficients (MFCC), neonatal seizure prediction,

¹Department of Electronic and Telecommunication Engineering, University of Moratuwa, Sri Lanka

²Department of Biomedical Engineering, University of Melbourne, Australia

³Department of Electrical and Computer Engineering, University of British Columbia, Canada

⁴Department of Pediatrics, Faculty of Medicine, University of Colombo, Sri Lanka

email: *ranasinghaasn.20@uom.lk, †pranjeevank@uom.lk

This work has been submitted to the IEEE for possible publication. Copyright may be transferred without notice, after which this version may no longer be accessible.

I. INTRODUCTION

Newborns, particularly during the first 28 days after birth (the neonatal period), are highly susceptible to seizures due to the immaturity of their central nervous system [1]. Epidemiological studies estimate that seizures occur in approximately 1-5.5 per 1000 live births in high-income countries and 1 to 39.5 per 1000 live births in middle-income and low-income countries (e.g. 4 per 1000 live births in Sri Lanka [2]) [3]. This probably reflects heavy underdiagnosis since the estimates were totally based on clinical observation of neonatal seizures. Early detection and intervention are critical, as neonatal seizures are associated with secondary brain injury and long-term neuro-developmental impairments [4].

Detecting or predicting neonatal seizures in the neonatal intensive care unit (NICU), based solely on clinical observation, is challenging, as seizures in this population often manifest with subtle or ambiguous symptoms and may be mistaken for normal infant behavior [5]. Currently, continuous video electroencephalogram (cEEG) monitoring is considered the gold standard for neonatal seizure detection [3]. Further, real-time seizure detection requires continuous expert supervision, making the process resource-intensive and often challenging in most clinical settings.

Electroencephalogram (EEG) signals recorded from babies with seizures are typically categorized into four states: interictal (normal brain activity), preictal (period preceding seizure onset), ictal (active seizure), and postictal (recovery period following seizure termination) (see Fig 1). While seizure detection focuses on identifying the ictal state, seizure prediction seeks to identify the preictal state to enable earlier intervention.

Recent studies have shown that machine learning models are capable of predicting seizures with over 90% accuracy while requiring minimal clinician input [6]–[8]. In addition to EEG, several studies indicate that electrocardiogram (ECG)-derived features can also provide useful information for seizure prediction [6], [9]. Furthermore, evidence suggests that integrating EEG and ECG can enhance neonatal seizure detection [10], while [7] recently proposed a model leveraging both EEG and ECG signals for seizure prediction in adult patients.

Seizure prediction approaches are usually categorized as patient-specific (trained and evaluated on one subject) or

patient-independent (trained on multiple subjects). Patient-specific models often yield higher accuracy for the specific subject, but are impractical in neonates because obtaining sufficient per-patient recordings for model training is difficult. Patient-independent models are more suitable for clinical deployment, yet their development is limited by substantial inter-subject variability in neonatal EEG signals, which constrains generalizability. As a result, patient-independent neonatal seizure prediction remains relatively underexplored compared to pediatric and adult populations.

To address this gap, we present a deep learning model capable of predicting neonatal seizures 30 minutes before onset, enabling timely clinical interventions. To the best of our knowledge, this is the *first study* to develop a deep learning-based framework for patient-independent prediction of neonatal seizures with explainability. Our method incorporates the following key features to enhance predictive performance and ensure applicability in real clinical settings.

- A *reduced-montage EEG for minimal clinical intrusiveness*.

By leveraging a reduced EEG electrode configuration, our approach eliminates the need for extensive scalp coverage in neonates, reducing discomfort and simplifying clinical setup without degrading performance.

- A *lightweight, multi-modal, and interpretable model, with an attention mechanism for enhanced feature relevance*.

Our model is computationally efficient, with only about 70k parameters, compared to 128k in [11], 289k in [8], and 2000k in [12] for state-of-the-art methods. The model fuses EEG and ECG signals with channel-wise attention to emphasize the most informative features, achieving robust performance across both neonatal and adult datasets. The model maintains high sensitivity and specificity while being lightweight, making it suitable for real-time clinical applications. In addition, we apply the SHapley Additive exPlanations (SHAP) explainable artificial intelligence (AI) technique to interpret the model, identifying the channels that contribute most to seizure prediction and thereby enhancing transparency, clinical interpretability, and enabling approximate localization of seizure onset.

In the following sections, we present the methodology and key outcomes of our study, demonstrating the strong performance of the proposed model under 10-fold cross-validation, and subject-wise leave-one-patient-out evaluation with transfer learning for neonatal seizure prediction.

II. RELATED WORK

Most existing seizure prediction methodologies are patient-specific, requiring access to prior EEG recordings from the same individual. While effective for the targeted subject, they often exhibit poor generalization to unseen patients due to substantial inter-subject variability in EEG patterns [11], [13]. This variability, combined with the scarcity of large, diverse clinical datasets, limits the development of patient-independent models.

Despite these challenges, recent work has focused on developing patient-independent models [11], [14]. Some studies have utilized domain adaptation techniques to improve

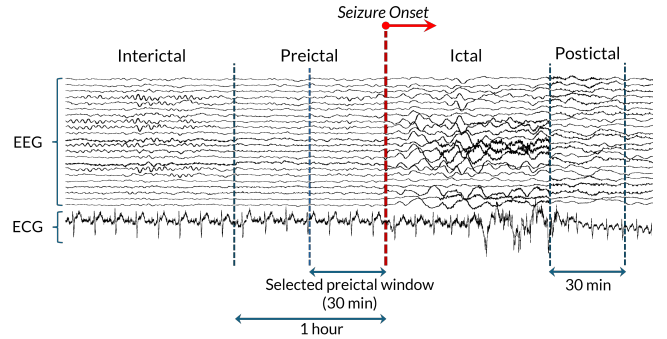


Fig. 1: **EEG and ECG recordings across four brain states associated with seizures.** The figure illustrates interictal, preictal, ictal, and postictal states, along with the respective time durations considered for Helsinki dataset construction in this study.

cross-subject performance [15], [16]. [11] proposed a convolutional neural network (CNN)-based patient-independent seizure prediction model incorporating contrastive learning to capture subject-specific patterns, achieving 91.54% accuracy and 0.9694 ROC-AUC on the CHB-MIT dataset [17], while [12] used a combination of features to train a CNN-based model, achieving 96% accuracy and 0.85 F1-score on the same dataset. Additionally, [8] developed a geometric deep learning model with attention mechanisms, achieving 95% accuracy and 0.99 ROC-AUC on the CHB-MIT dataset [17], and 96% accuracy with 0.99 ROC-AUC on the Siena dataset [18].

To support both patient-specific and patient-independent models, most studies extract conventional features such as statistical moments [19], [20], entropy measures [19], short-time Fourier transform (STFT) [21], [22], discrete wavelet transforms [6], [14], and intrinsic mode function (IMF) based features [23]. [20] further employed graph-theoretic features. Additionally, studies show that mel-frequency cepstral coefficients (MFCCs), originally developed for audio signal processing, possess strong capabilities for capturing generalized seizure patterns [8], [11], [12].

After feature extraction, studies have employed classifiers ranging from conventional K-Nearest Neighbors (KNN) [6], to more advanced architectures such as long short-term memory (LSTM) networks [19], [20], [24], CNNs [14], [16], [25], and transformer-based models [22], [26], with LSTMs and CNNs consistently demonstrating strong predictive performance.

As these models become increasingly complex, understanding their decision-making is critical for clinical adoption. The inherent black-box nature of deep learning models poses challenges in this regard. Recent studies have incorporated interpretability techniques such as SHAP [11], logistic regression-based interpretations [27], and model transparency frameworks [28], enabling clinicians to understand predictions and build trust in AI-assisted diagnosis.

Despite the advancements, most existing research has focused only on pediatric and/or adult populations, and are mostly patient-specific. Patient-independent seizure prediction in neonates with clinical interpretability remains largely unexplored and represents a critical gap in the current literature.

III. DATA PREPARATION

A. Datasets

This study primarily utilized two publicly available datasets: the Helsinki neonatal EEG-ECG dataset from Helsinki University Hospital [29], and the Siena scalp EEG-ECG dataset [18]. Additionally, we also trained and evaluated our model using the CHB-MIT [17] dataset; however, this dataset does not contain ECG and also does not allow us selection of the nine electrodes we use in this study.

The Helsinki dataset [29] comprises multi-channel EEG and ECG recordings from 79 term neonates admitted to the NICU of Helsinki University Hospital. EEG recordings were independently annotated by three clinical experts, with an average of 460 annotated seizures per expert. Based on consensus annotations, 39 neonates were identified as having seizures, while 22 were seizure-free. All recordings were acquired at a sampling rate of 256 Hz with 21 electrodes positioned according to the international 10–20 EEG system [29]. Out of the 39 neonates with seizures, we first identified those with consistently annotated seizure events across all three experts. From this subset, the dataset was constructed according to the preprocessing procedure and the definitions of preictal, interictal, and postictal states described in Section III-B. To ensure the suitability of the dataset for binary classification, we further restricted the selection to neonates who had data from both the interictal and preictal classes. This step was necessary because, in typical deep learning-based binary classification frameworks, the presence of both classes for each subject is critical to avoid biased learning and to allow the model to generalize across conditions. After applying these criteria, the final dataset comprised 9 neonates who were the only ones who fulfilled all inclusion requirements.

The Siena dataset [18] comprises EEG and ECG recordings from 14 epileptic adults, collected at the Unit of Neurology and Neurophysiology, University of Siena. The recordings were acquired using the international 10–20 electrode placement system at a sampling rate of 512 Hz and include a total of 47 seizure events. To reduce computational complexity, all signals were downsampled by a factor of two during preprocessing.

Both datasets provide electrode-wise EEG potentials. In the Helsinki dataset, recordings are referenced to the Cz electrode, whereas the Siena dataset does not specify the reference. From each dataset, signals were selected from nine electrodes using a reduced montage electrode configuration and 18 EEG channel combinations were constructed. Twelve of these channels were selected following the methodology used in [30], while six additional channels were included to capture frontal-central, central-occipital, and cross-hemisphere potentials, potentially improving predictive performance. The final set of EEG channel pairs included: Fp1-T3, T3-O1, Fp1-C3, C3-O1, Fp2-C4, C4-O2, Fp2-T4, T4-O2, T3-C3, C3-Cz, Cz-C4, C4-T4, Fp1-Cz, Cz-O1, Fp2-Cz, Cz-O2, Fp1-O2, and Fp2-O1 (see Fig 2).

The CHB-MIT dataset, in contrast, contains EEG recordings from 22 pediatric subjects, acquired at a sampling frequency of 256 Hz. This dataset already contains bipolar EEG channels

that are different to the bipolar channels that were constructed for the other two datasets in this study. Most subjects have 23 EEG channels, while a minority have slightly fewer or more. To maintain consistency with previous studies, we standardized the input to 23 channels. For patients with only 22 available channels, an additional channel was generated by averaging existing channels, following the approach described in [8], [11], [12].

B. Preprocessing

To remove baseline drift and high-frequency noise while preserving signal components relevant to seizure prediction, we applied a 4th-order Butterworth infinite impulse response (IIR) bandpass filter with a passband of 0.1 Hz–70 Hz to both EEG and ECG signals, following the approach in [7]. Additionally, a 4th-order Butterworth IIR notch filter at 50 Hz was applied to eliminate power line interference.

There is no standard duration for the preictal stage preceding seizure onset [31]. Previous studies have adopted varying durations depending on dataset characteristics and experimental design, with 30 minutes and 1 hour being the most commonly used [8], [11], [12]. Due to the limited non-seizure data of epileptic patients in the Helsinki dataset, we defined the preictal period as the 30 minutes preceding a seizure, assuming it ends just before seizure onset, and the postictal period as the 30 minutes following seizure termination. Interictal segments were selected from at least one hour prior to seizure onset (see Fig 1). All signals were then segmented into non-overlapping 5-second windows.

To ensure consistency in evaluation, we adopted the methodology described in [8] when selecting preictal and interictal samples from the Siena and the CHB-MIT datasets. The preictal period was defined as 1 hour in duration, whereas interictal samples were selected at least 4 hours before seizure onset in the CHB-MIT dataset and at least 1 hour before in the Siena dataset. These segments were also divided into 5-second non-overlapping windows to align with the segmentation used for the Helsinki dataset.

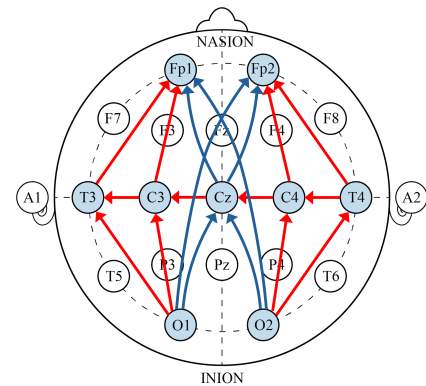


Fig. 2: **Scalp electrode placement and EEG channel selection.** Electrodes selected for this study are shaded in blue. Red and blue arrows indicate the EEG channels: red arrows correspond to the twelve channels defined in [30], while blue arrows denote the six additional channels introduced in this study.

C. MFCC Calculation

Although originally developed for speech processing, MFCCs have demonstrated efficacy in EEG-based seizure prediction tasks [8], [11], [12], [32]. In this study, MFCCs are used as input features due to their ability to capture discriminative spectral patterns associated with the preictal stage.

The MFCC computation process comprises five key steps: (1) segmenting the signal into overlapping time frames and applying a Hamming window to minimize spectral leakage, (2) computing the magnitude spectrum via fast Fourier transform, (3) applying a triangular mel-filter bank, (4) performing a logarithmic transformation on the filter bank energies, and (5) applying the discrete cosine transform to decorrelate features and retain the most informative coefficients.

We employed the open-source Torchaudio library [33], [34] to compute MFCC matrices from multichannel EEG and ECG signals. A hop length of 128 was used, yielding 11 time frames for each 5-second interictal and preictal segment. Twenty mel filter banks were constructed to span the 0.5-100 Hz frequency range. Following the data-level fusion strategy presented in [7], multi-channel EEG and ECG data were stacked along the channel dimension. Consequently, each MFCC feature matrix had dimensions of (19, 20, 11), where 19 corresponds to the total number of EEG and ECG channels. These matrices served as inputs to the seizure prediction model.

IV. PROPOSED MODEL ARCHITECTURE

This section outlines the architecture of our proposed neonatal seizure prediction model, which comprises three primary components: (1) a CNN encoder, (2) a channel attention mechanism, and (3) a classifier for seizure prediction. The input to the model is a multichannel MFCC matrix derived from EEG and ECG signals. These MFCC representations are initially processed by a three-layer 2D-CNN encoder. The resulting feature embeddings are then passed through a channel attention block, which adaptively assigns weights to each channel based on its relevance to seizure prediction. Finally, the weighted embeddings are fed into a fully connected layer to classify each segment as either interictal or preictal. The model was designed to be lightweight, with a low number of parameters, while allowing for interpretability. Fig. 3 illustrates the overall pipeline and architecture of the proposed model. Table I presents a comparison of our model with state-of-the-art methods in terms of the number of model parameters.

A. CNN Encoder

The CNN encoder is composed of three sequential 2D convolutional blocks. Each block includes a 2D convolutional layer, followed by batch normalization, a ReLU activation, dropout, and max-pooling. The convolutional layers use 32, 64, and 128 filters in the first, second, and third blocks, respectively.

Batch normalization is applied after each convolution to stabilize the training process and mitigate the risk of gradient

explosion. A dropout layer follows each block to prevent overfitting by randomly deactivating a subset of neurons during training. Max-pooling with a kernel size of (2, 2) is used at the end of each block to progressively reduce the spatial dimensions, retain salient features, and lower computational complexity. The resulting feature maps from the final convolutional block are passed to the channel attention mechanism.

B. Squeeze-and-Excitation Channel Attention

To enhance the model's ability to focus on the most informative feature channels, we integrate the squeeze-and-excitation (SE) attention mechanism proposed in [35]. This mechanism adaptively recalibrates channel-wise feature responses by explicitly modeling inter-channel dependencies based on global contextual information.

Let the input feature map be denoted by $\mathbf{X} \in \mathbb{R}^{C \times H \times W}$, where C is the number of channels, and H and W are the spatial dimensions. The SE block consists of three main stages: squeeze, excitation, and recalibration.

1) Squeeze: A global average pooling operation is applied across each spatial dimension to generate a channel-wise descriptor $\mathbf{z} \in \mathbb{R}^C$:

$$z_c = \frac{1}{H \times W} \sum_{i=1}^H \sum_{j=1}^W X_c(i, j), \quad \forall c \in \{1, \dots, C\} \quad (1)$$

2) Excitation: The descriptor \mathbf{z} is passed through a bottleneck structure comprising two convolutional layers with a kernel size of 1. The first layer reduces the dimensionality by a factor of r , which is tunable in our study, and applies a ReLU activation. The second layer restores the original dimension and applies a sigmoid activation to produce normalized attention weights $\mathbf{s} \in \mathbb{R}^C$:

$$\mathbf{s} = \sigma(\mathbf{W}_2 \delta(\mathbf{W}_1 \mathbf{z})) \quad (2)$$

Here, $\delta(\cdot)$ denotes the ReLU activation function, $\sigma(\cdot)$ is the sigmoid function, and $\mathbf{W}_1 \in \mathbb{R}^{\frac{C}{r} \times C}$, $\mathbf{W}_2 \in \mathbb{R}^{C \times \frac{C}{r}}$ are learnable parameters corresponding to the two convolutional layers.

3) Recalibration: The resulting attention weights \mathbf{s} are broadcast and applied to the original feature map via channel-wise multiplication to emphasize informative channels.

$$\tilde{\mathbf{X}}_c = s_c \cdot \mathbf{X}_c, \quad \forall c \in \{1, \dots, C\} \quad (3)$$

The recalibrated output $\tilde{\mathbf{X}} \in \mathbb{R}^{C \times H \times W}$ is then passed to the subsequent layers of the model. This mechanism allows the network to selectively amplify informative features while suppressing less relevant ones, thereby improving its discriminative capability for seizure prediction.

C. Classifier

The final component of the proposed model is a fully connected classifier. The attention-weighted feature maps are first flattened into a one-dimensional vector and passed through a

fully connected layer comprising 128 neurons. A sigmoid activation function is then applied to generate a probability score that reflects the likelihood of the input segment corresponding to a preictal state. During inference, a fixed threshold of 0.5 is used to convert this probability into a binary class label, with values greater than or equal to the threshold classified as preictal and the remainder as interictal.

TABLE I: Comparison of the number of learnable parameters between the proposed model and existing patient-independent seizure prediction models.

Work	No. of Parameters
Dissanayake et al. [11]	128k
Dissanayake et al. [8]	289k
Zhang et al. [12]	2000k
Ours	70k

V. MODEL TRAINING AND INTERPRETATION

A. 10-Fold Cross-Validation

To assess the robustness and reliability of the proposed model, we employed 10-fold cross-validation. The model was trained using the binary cross-entropy loss function and optimized with the Adam optimizer. To reduce overfitting, dropout and weight decay regularization were applied. In addition, a Reduce-on-Plateau learning rate scheduler was used, with patience, factor, and minimum learning rate set to 25, 0.98, and 10^{-7} , respectively, to facilitate better convergence by reducing the learning rate when the validation loss plateaued. Furthermore, class weights were incorporated into the loss function to address class imbalance in the datasets.

TABLE II: Hyper-parameter settings used for model training on each dataset.

Hyper-parameter	Helsinki	Siena	CHB-MIT
Learning rate	0.0004	0.002	0.0002
Batch size	256	128	128
Weight decay	0.005	0.0001	0.0001
Dropout	0.3	0.0001	0.2
Positive class weight	0.52	0.51	0.5
Reduction factor	8	16	32

The key hyper-parameters, including learning rate, dropout probability, weight decay, training batch size, positive class weight factor, and reduction factor in the attention layer, were tuned via random search. Table II presents the hyperparameter values selected based on the results.

Model performance was monitored throughout training and evaluation using multiple metrics, including accuracy, sensitivity, specificity, and F1-score, to ensure a comprehensive assessment of predictive capability.

B. Leave-One-Patient-Out Evaluation

In addition to 10-fold cross-validation, we conducted a leave-one-patient-out (LOPO) evaluation to examine the model’s generalization capability. Here the model is trained

using all available neonates except one neonate and evaluated on that held-out neonate. Given the limited number of subjects in the Helsinki dataset, the generalization to unseen patients posed a challenge due to high inter-subject variability.

To address this issue, we adopted a transfer learning approach. The model was initially trained on data from all available neonates except the target subject. It was then fine-tuned using a short-duration signal segment comprising both interictal and preictal samples from the held-out neonate. We fine-tuned the pre-trained model using two sample sizes. First, we used 12 consecutive preictal samples (1 minute) from the beginning of the preictal period of the first available seizure for each neonate, along with 12 randomly selected interictal samples (each 5 seconds long). Second, we used 60 samples from each class following the same procedure. Consecutive preictal samples were chosen from the start of the defined preictal period to evaluate the model’s ability to detect preictal patterns distant from seizure onset and thereby predict upcoming seizures with sufficient lead time for clinical intervention.

C. Model Interpretation

To improve the interpretability of model predictions, we used the SHAP explainable AI algorithm introduced in [36]. First, we constructed a test set comprising the first six preictal segments from the beginning of the preictal period of the earliest seizure for which preictal samples could be extracted for each neonate, following the method described in Section III-B. We then randomly selected six interictal segments from each neonate. This approach was designed to identify the EEG channels that initially exhibit abnormal activity, while minimizing overlap with channels affected as the seizure propagates, thereby facilitating the localization of the seizure focus. After retraining the model on the remaining data (70% for training, 30% for validation), SHAP values for the test set were computed to assess signal channel contributions.

For each input of shape (19, 20, 11), the SHAP algorithm produces a matrix of identical dimensions. The resulting SHAP values can be positive or negative, with the sign indicating whether the contribution of the corresponding input element increases or decreases the model output for the positive class (in our case, the preictal class). To localize the focus of the seizures for each neonate, we calculated the average of the first three preictal SHAP matrices of that neonate, providing a more robust estimate. The channel-wise SHAP values for each neonate were then obtained using the following formula. Let \mathbf{c} denote the signal channel, $\mathbf{S}_c \in \mathbb{R}^{20 \times 11}$ represent the SHAP matrix ($\in \mathbb{R}^{20 \times 11}$) of channel \mathbf{c} obtained from the averaged 3D SHAP matrix ($\in \mathbb{R}^{19 \times 20 \times 11}$), and $\mathbf{I} \in \mathbb{R}^{19 \times 1}$ represent the resulting channel-wise importance.

$$I_c = \frac{\mu_{S_c}}{\sigma_{S_c}}, \quad c \in \{1, \dots, 19\} \quad (4)$$

Here, μ and σ denote the mean and standard deviation, respectively.

To select the channels that contribute to a positive prediction, we retained only those with positive importance

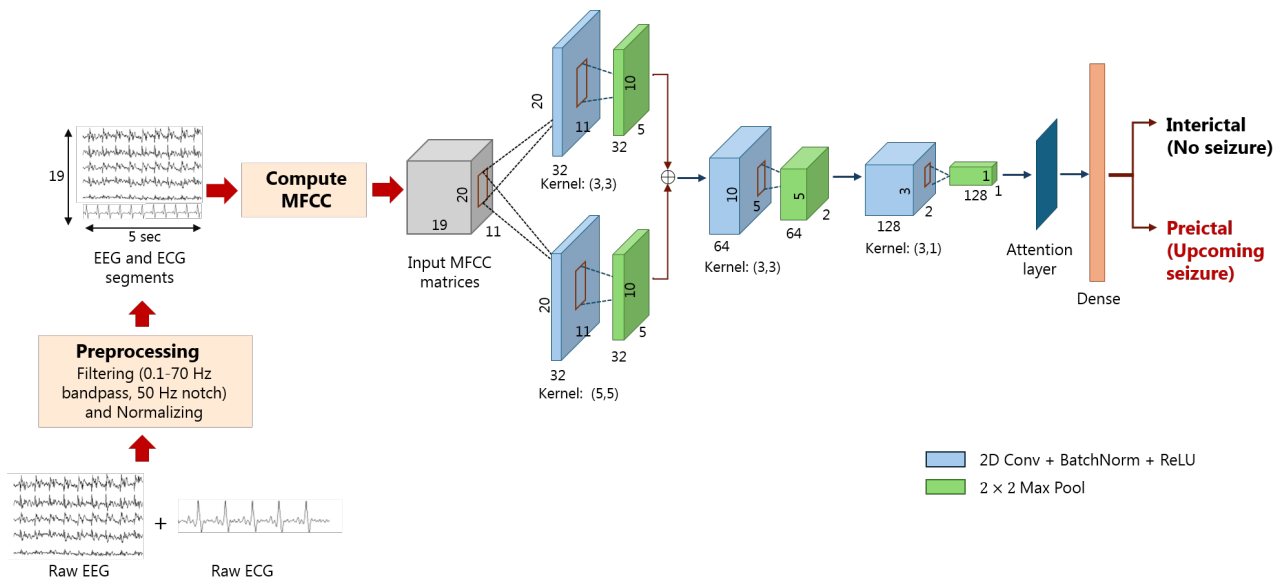


Fig. 3: Architecture of the proposed deep learning model for seizure prediction. Raw EEG and ECG are preprocessed, segmented into 5 s windows, and converted into MFCC matrices. Features are extracted using 2D convolutional layers with batch normalization and ReLU (blue) and max pooling layers (green). An attention mechanism precedes the dense classifier, which produces a binary output: 1 for preictal (upcoming seizure) and 0 for interictal (no seizure).

values and set all other channel importance values to zero. We then excluded the ECG channel importance and performed min-max normalization on the resulting importance array of shape $\mathbb{R}^{18 \times 1}$, to map values to the $[0, 1]$ range for better visualization.

All code used for our work is publicly available at <https://github.com/Sithminii/BraiNeoCare>.

VI. RESULTS AND DISCUSSION

A. 10-Fold Cross-Validation Results

We conducted 10-fold cross-validation over three independent trials to ensure the robustness and reproducibility of our results. Table III presents the average performance metrics across these trials, along with results from patient-independent state-of-the-art methods for reference.

To further evaluate the contributions of the attention mechanism and the ECG input to seizure prediction performance, we performed an ablation study. This analysis involved conducting 10-fold cross-validation for three different preictal durations, 30, 15, and 10 minutes. For each duration, experiments were performed both with and without the attention layer, and in each case, the model’s performance was evaluated with and without ECG as an input modality. The results of this ablation analysis are summarized in Table IV.

As shown in Table III, our method achieved performance comparable to that of [8] on the Siena dataset, while demonstrating superior accuracy and sensitivity. On the CHB-MIT dataset, performance was lower than that of [8], [11] and [12]. This discrepancy can be attributed to several factors. First, in both the Helsinki and Siena datasets, we constructed a consistent 18-channel EEG montage, since the recordings were referenced to a common electrode. In contrast, the CHB-MIT

dataset does not provide a common reference and channels are already pre-defined, preventing us from reproducing the same 18-channel configuration and requiring us to use the available 23 channels instead. Second, unlike the Helsinki and Siena datasets, the CHB-MIT dataset does not include ECG recordings, which formed a complementary input modality in our proposed seizure prediction framework. Third, several previous studies have generated preictal samples using overlapping segments, which can introduce information leakage between training and validation sets. In contrast, we employed non-overlapping 5-second segments. Given our relatively short segment length, introducing overlap would have substantially increased redundancy and the risk of leakage and therefore, we opted for strictly non-overlapping windows to obtain a more conservative and realistic estimate of model performance. Finally, our model and preprocessing strategies were primarily optimized for neonatal recordings and generalized well to adult data, but pediatric EEG characteristics may differ in ways that could reduce performance relative to the other two populations.

Our method achieved over 96% and 95% in accuracy, sensitivity, specificity, and F1-score on the Helsinki and Siena datasets, respectively, with an average ROC-AUC of 0.99 on both, demonstrating the model’s capability to detect impending seizures at least 30 minutes and one hour before onset in neonates and adults, respectively.

As shown in Table IV, for the 30-minute preictal duration, integrating ECG signals and incorporating the attention layer improved model performance. However, for the 10-minute and 15-minute preictal durations, higher values across different performance metrics were observed for different combinations of attention presence and input modalities (EEG only or EEG and ECG both). No single combination consistently

TABLE III: Performance comparison between our method and state-of-the-art methods. For each dataset, the highest value for each evaluation metric across all methods is highlighted in bold.

Work	Dataset	Input	Acc (%)	Sen (%)	Spec (%)	F1-score (%)
Dissanayake et al. [11]	CHB-MIT	EEG	91.54 ± 0.17	92.45 ± 0.22	89.94 ± 0.21	-
Dissanayake et al. [8]	Siena	EEG	96.05 ± 0.17	96.05 ± 0.17	96.61 ± 0.20	-
Zhang et al. [12]	CHB-MIT	EEG	96	92	84	85
Ours	Helsinki (30 min)	EEG	96.23 ± 0.20	96.65 ± 0.18	95.58 ± 0.29	96.86 ± 0.17
		EEG + ECG	97.52 ± 0.04	98.31 ± 0.21	96.39 ± 0.33	97.95 ± 0.03
	Siena	EEG	95.60 ± 0.09	96.17 ± 0.15	95.02 ± 0.06	95.62 ± 0.09
		EEG + ECG	96.57 ± 0.05	97.31 ± 0.01	95.84 ± 0.12	96.60 ± 0.05
CHB-MIT	EEG	85.18 ± 0.70	86.40 ± 3.03	83.96 ± 1.62	85.30 ± 1.03	

TABLE IV: 10-fold cross-validation results on the Helsinki dataset for the proposed model, without ECG and without attention.

Duration	Input	Performance Metrics				
		Acc (%)	Sen (%)	Spec (%)	F1-score (%)	
30 min	No attention	EEG	95.25 ± 0.08	96.99 ± 0.28	92.55 ± 0.58	96.10 ± 0.07
		EEG + ECG	96.96 ± 0.05	97.12 ± 0.20	96.74 ± 0.15	97.46 ± 0.05
	Attention	EEG	96.23 ± 0.20	96.65 ± 0.18	95.58 ± 0.29	96.86 ± 0.17
		EEG + ECG	97.52 ± 0.04	98.31 ± 0.21	96.39 ± 0.33	97.95 ± 0.03
15 min	No attention	EEG	97.52 ± 0.15	97.62 ± 0.07	97.45 ± 0.21	97.22 ± 0.17
		EEG + ECG	97.25 ± 0.04	97.51 ± 0.23	97.05 ± 0.17	96.93 ± 0.04
	Attention	EEG	96.60 ± 0.38	98.46 ± 0.33	95.11 ± 0.96	96.28 ± 0.36
		EEG + ECG	97.41 ± 0.05	97.20 ± 0.20	97.59 ± 0.10	97.11 ± 0.06
10 min	No attention	EEG	97.94 ± 0.11	97.92 ± 0.27	97.97 ± 0.03	97.10 ± 0.15
		EEG + ECG	97.95 ± 0.50	98.68 ± 0.24	97.55 ± 0.77	97.18 ± 0.63
	Attention	EEG	98.10 ± 0.12	98.24 ± 0.11	98.02 ± 0.13	97.32 ± 0.16
		EEG + ECG	97.99 ± 0.07	97.83 ± 0.24	98.08 ± 0.16	97.17 ± 0.11

outperformed the others across all four metrics for the 10-minute and 15-minute durations. For the 30-minute preictal duration, incorporating both EEG and ECG data resulted in an approximate 1.42% improvement in F1-score compared with using EEG alone without attention, suggesting that ECG signals contained complementary seizure-related information that enhanced predictive performance. Furthermore, integrating attention mechanisms provided an additional 0.5% improvement in F1-score, underscoring the benefit of emphasizing salient features during learning.

B. Leave-One-Patient-Out Results

In addition to 10-fold cross-validation, we performed LOPO cross-validation to evaluate the generalization capability of our model on completely unseen neonates. Given the high inter-subject variability in EEG patterns, we observed that the model struggled to reliably distinguish between interictal and preictal segments when evaluated directly on data from an unseen subject. The average accuracy, sensitivity, specificity, and F1-score across nine neonates using LOPO cross-validation were 58.47%, 58.53%, 58.14%, and 60.28%, respectively. Accordingly, as previously described, we employed a transfer learning strategy in which the entire model was fine-tuned using a limited set of samples from the previously unseen subject. The model’s performance in LOPO for each neonate, along with the fine-tuned results for two different fine-tuning dataset sizes, is presented in Table V.

According to Table V, the pre-trained model demonstrated

consistent improvements across all four evaluation metrics following fine-tuning with a very small number of samples. Previous studies, such as [11], have also explored fine-tuning strategies and reported promising results, primarily in terms of accuracy. In contrast, by incorporating additional evaluation metrics such as the F1-score, our analysis provides a more comprehensive assessment of model performance. Notably, while earlier work relied on larger sample sizes for fine-tuning, our findings suggest that high performance, exceeding approximately 90% across all metrics, can be achieved with considerably fewer samples. When fine-tuned using only 1 minute of data from each interictal and preictal state (N=24), the model achieved average accuracy, sensitivity, specificity, and F1-score of 81.55%, 80.89%, 84.54%, and 84.89%, respectively. With 5 minutes of data from each state (N=120), these values increased to 94.85%, 95.25%, 96.78%, and 95.88%, respectively. The ability to achieve strong performance with fine-tuning on short-duration data is particularly relevant in clinical contexts, as it highlights the feasibility of adapting the model efficiently to neonatal data, which often comes with limited availability. However, although both studies investigate the prediction of seizures, differences in target cohorts, pediatric versus neonatal, limit the possibility of a direct comparison.

C. Model Interpretation

For each neonate, the processed channel importances are mapped onto the scalp electrode map and presented in Fig. 4. The recorded seizure locations from the Helsinki dataset are

TABLE V: Subject-wise leave-one-patient-out (LOPO) results and fine-tuned performance for each neonate using two sample sizes: $N = 24$ and $N = 120$.

Neonate ID	LOPO				$N = 24$ (Int: 1 min, Pre: 1 min)				$N = 120$ (Int: 5 min, Pre: 5 min)			
	Acc (%)	Sen (%)	Spec (%)	F1-Score (%)	Acc (%)	Sen (%)	Spec (%)	F1-Score (%)	Acc (%)	Sen (%)	Spec (%)	F1-Score (%)
11	71.92	65.65	75.90	64.37	95.57	93.10	97.12	94.19	95.66	93.33	97.04	94.12
13	56.83	36.20	77.17	42.83	83.45	86.78	80.17	83.89	91.90	91.00	92.79	91.76
15	62.09	62.13	61.98	70.39	70.04	64.66	86.21	76.40	100	100	100	100
21	65.71	66.25	64.33	73.43	70.98	75.00	60.31	78.97	99.48	99.67	99.33	100
40	46.38	49.07	19.45	57.26	74.19	72.70	95.83	84.05	90.00	99.04	100	99.50
51	71.84	76.48	58.97	79.93	83.05	82.47	84.75	87.90	91.35	92.67	85.71	94.56
62	60.64	64.90	58.28	55.79	98.94	97.00	100	98.48	100	100	100	100
66	45.67	43.98	69.00	58.93	70.42	70.62	68.49	81.23	89.93	89.55	100	94.48
77	45.12	62.12	38.17	39.60	87.32	85.71	87.94	78.87	95.37	92.00	96.17	88.46
Average	58.47	58.53	58.14	60.28	81.55	80.89	84.54	84.89	94.85	95.25	96.78	95.88

reported under the corresponding scalp map of each neonate. Each linear connection between two electrodes represents the corresponding EEG channel among the 18 channels used in this study. Darker connections indicate higher-importance channels, while lighter connections correspond to lower-importance channels.

According to Fig 4, for the majority of neonates (Neonates 13, 15, 51, 62, 66, and 77), the possible locations of seizures based on scalp maps align with the actual locations of seizures reported in the Helsinki dataset. In these cases, the predominant channels identified through processed SHAP importances are located at, or in close proximity to, the actual seizure locations reported in the clinical records. These scalp plots therefore, serve not only as a valuable interpretability tool but also as a clear visualization of the model's decision-making process, providing clinicians with an exact or approximate localization of seizure focus while enhancing the overall transparency of the predictive framework.

The scalp maps of neonates 11, 21, and 40 show slightly deviated seizure locations compared to their actual locations. For Neonate 11, clinical data indicate that the primary seizure location is in the right posterior quadrant of the scalp. However, as shown in Fig. 4a, more predominant channels are observed in the left hemisphere, while notable activation is also present in the right posterior quadrant. The scalp map of Neonate 21 (see Fig. 4d) shows several high-importance EEG channels in the left hemisphere, in addition to the right hemisphere, which is reported in the dataset as the primary seizure location for this neonate. Also, the scalp map of Neonate 40 (see Fig. 4c) shows high-importance channels predominantly in the right hemisphere, with no visibly important channels in the left occipital region. Notably, high-importance channels are observed in the left parietal region, indicating partial alignment with the reported seizure location for this neonate. These slight deviations may arise because the actual preictal onset begins earlier than the preictal interval considered in this study, allowing propagated activity to be recorded by neighboring channels. However, the scalp plots of these three neonates still show partial alignment with the clinical seizure focus and may provide clinicians with complementary insights for seizure localization.

VII. CONCLUSION

In this study, we addressed a significant research gap by developing a patient-independent seizure prediction model leveraging EEG and ECG signals for enhanced performance.

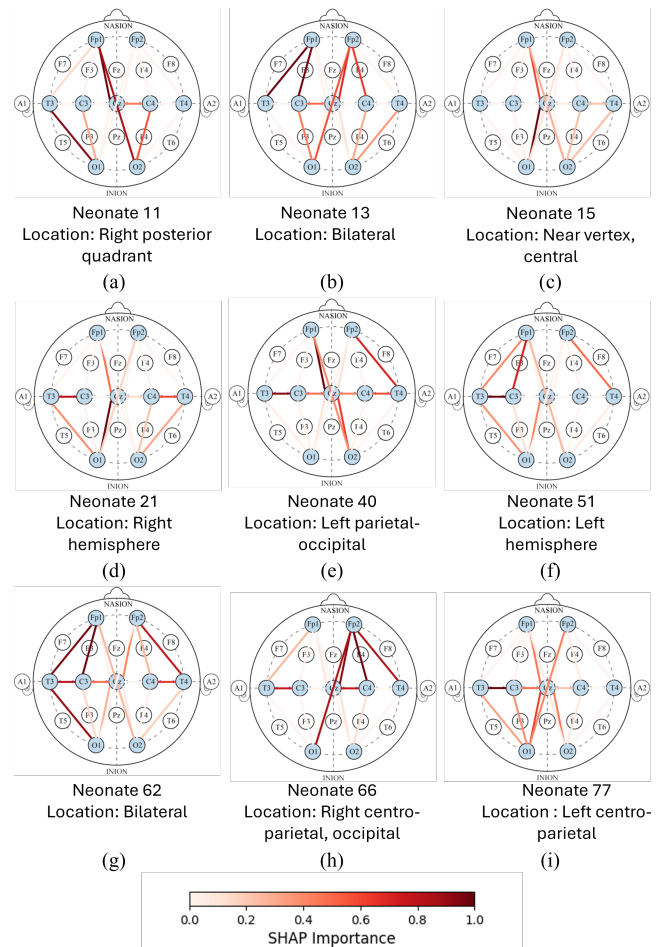


Fig. 4: Scalp Mapping of SHAP Values for Preictal EEG Samples in Neonates. The primary seizure location is indicated below each plot. Shaded electrodes highlight the nine electrodes used in this study, while lines between electrode pairs represent the 18 EEG channels. Line intensity corresponds to SHAP-based importance, with darker lines indicating greater importance.

We proposed a lightweight CNN-based model integrated with attention mechanisms, which was trained and validated on the Helsinki neonatal dataset, yielding promising results and advancing the field of neonatal seizure prediction. By fine-tuning with only a few samples, our method can generalize well to new subjects, demonstrating its applicability in real-world clinical settings. Our approach incorporates explainable AI techniques, generating scalp plots based on model predictions to help clinicians understand and localize upcoming seizures, enabling timely interventions and improved neonatal care. While further research with larger datasets is needed to enhance generalization and clinical applicability, our results provide a strong foundation for future studies and highlight the potential of AI-driven seizure prediction to improve neonatal outcomes.

ACKNOWLEDGMENT

The computational resources used in this project were funded by the Clair Accelerating Higher Education Expansion and Development (AHEAD) Operation of the Ministry of Higher Education of Sri Lanka, funded by the World Bank.

- [1] J. Kim, S. Yoo, C. Liu, S. S. Kwak, J. R. Walter, S. Xu, and J. A. Rogers, "Skin-interfaced wireless biosensors for perinatal and paediatric health," *Nature Reviews Bioengineering*, vol. 1, no. 9, pp. 631–647, Jul. 2023. [Online]. Available: <https://doi.org/10.1038/s44222-023-00090-0>
- [2] J. Wanigasinghe, "Seizures in small brains," *Sri Lanka Journal of Neurology*, vol. 11, no. 1, pp. 3–8, 8 2024. [Online]. Available: <https://doi.org/10.4038/sljon.v11i1.174>
- [3] M. A. J. Ryan and A. Malhotra, "Electrographic monitoring for seizure detection in the neonatal unit: current status and future direction," *Pediatric Research*, vol. 96, no. 4, pp. 896–904, Apr. 2024. [Online]. Available: <https://doi.org/10.1038/s41390-024-03207-2>
- [4] B. Maimaiti, H. Meng, Y. Lv, J. Qiu, Z. Zhu, Y. Xie, Y. Li, N. Yu-Cheng, W. Zhao, J. Liu, and M. Li, "An Overview of EEG-based Machine Learning Methods in Seizure Prediction and Opportunities for Neurologists in this Field," *Neuroscience*, vol. 481, pp. 197–218, Nov. 2021. [Online]. Available: <https://doi.org/10.1016/j.neuroscience.2021.11.017>
- [5] E. M. Mizrahi and P. Kellaway, "Characterization and classification of neonatal seizures," *Neurology*, vol. 37, no. 12, p. 1837, Dec. 1987. [Online]. Available: <https://doi.org/10.1212/wnl.37.12.1837>
- [6] A. V. Perez-Sanchez, J. P. Amezcua-Sanchez, M. Valtierra-Rodríguez, and H. Adeli, "A new epileptic seizure prediction model based on maximal overlap discrete wavelet packet transform, homogeneity index, and machine learning using ECG signals," *Biomed. Signal Process. Control.*, vol. 88, p. 105659, 2024. [Online]. Available: <https://api.semanticscholar.org/CorpusID:265028748>
- [7] Y. Yang, X. Qin, H. Wen, F. Li, and X. Lin, "Patient-specific approach using data fusion and adversarial training for epileptic seizure prediction," *Frontiers in Computational Neuroscience*, vol. 17, 5 2023. [Online]. Available: <https://doi.org/10.3389/fncom.2023.1172987>
- [8] T. Dissanayake, T. Fernando, S. Denman, S. Sridharan, and C. Fookes, "Geometric deep learning for subject independent epileptic seizure prediction using scalp EEG signals," *IEEE Journal of Biomedical and Health Informatics*, vol. 26, no. 2, pp. 527–538, 2022.
- [9] F. Mason, A. Scarabello, L. Taruffi, E. Pasini, G. Calandra-Buonaura, L. Vignatelli, and F. Bisulli, "Heart rate variability as a tool for seizure prediction: A scoping review," *J. Clin. Med.*, vol. 13, no. 3, p. 747, 2024. [Online]. Available: <https://doi.org/10.3390/jcm13030747>
- [10] M. Malarvili and M. Mesbah, "Combining newborn EEG and HRV information for automatic seizure detection," in *Annu Int Conf IEEE Eng Med Biol Soc*, 2008, pp. 4756–4759.
- [11] T. Dissanayake, T. Fernando, S. Denman, S. Sridharan, and C. Fookes, "Deep learning for patient-independent epileptic seizure prediction using scalp EEG signals," *IEEE Sensors Journal*, vol. 21, pp. 9377–9388, 2021. [Online]. Available: <https://api.semanticscholar.org/CorpusID:232151780>
- [12] F. Zhang, B. Zhang, S. Guo, and X. Zhang, "MFCC-CNN: A patient-independent seizure prediction model," *Neurological Sciences*, vol. 45, no. 12, pp. 5897–5908, 8 2024. [Online]. Available: <https://doi.org/10.1007/s10072-024-07718-y>
- [13] Y. Roy, H. Banville, I. Albuquerque, A. Gramfort, T. H. Falk, and J. Faubert, "Deep learning-based electroencephalography analysis: a systematic review," *Journal of Neural Engineering*, vol. 16, no. 5, p. 051001, 2019, systematic Review. [Online]. Available: <https://doi.org/10.1088/1741-2552/ab260c>
- [14] R. I. Halawa, S. M. Youssef, and M. N. Elagamy, "An efficient hybrid model for patient-independent seizure prediction using deep learning," *Applied Sciences*, 2022. [Online]. Available: <https://api.semanticscholar.org/CorpusID:249173139>
- [15] Y. Zhao, S. Feng, C. Li, R. Song, D. Liang, and X. Chen, "Source-free domain adaptation for privacy-preserving seizure prediction," *IEEE Transactions on Industrial Informatics*, vol. 20, pp. 2787–2798, 2024. [Online]. Available: <https://api.semanticscholar.org/CorpusID:260412519>
- [16] I. Jemal, L. Abou-Abbas, K. Henni, A. Mitiche, and N. Mezghani, "Domain adaptation for EEG-based, cross-subject epileptic seizure prediction," *Frontiers in Neuroinformatics*, vol. 18, 2024. [Online]. Available: <https://api.semanticscholar.org/CorpusID:267416573>
- [17] J. Gutttag, "CHB-MIT Scalp EEG Database (version 1.0.0)," <https://doi.org/10.13026/C2K01R>, 2010, available at: <https://doi.org/10.13026/C2K01R>.
- [18] P. Detti, G. Vatti, and G. Zabalo Manrique de Lara, "EEG synchronization analysis for seizure prediction: A study on data of noninvasive recordings," *Processes*, vol. 8, no. 7, 2020. [Online]. Available: <https://www.mdpi.com/2227-9717/8/7/846>
- [19] I. Ahmad, M. Zhu, Z. Liu, M. Shabaz, I. Ullah, M. C. F. Tong, A. Sambas, L. Men, Y. Chen, and S. Chen, "Multi-feature fusion based convolutional neural networks for EEG epileptic seizure prediction in consumer internet of things," *IEEE Transactions on Consumer Electronics*, 2024. [Online]. Available: <https://api.semanticscholar.org/CorpusID:267559957>
- [20] K. M. Tsiouris, V. C. Pezoulas, M. E. Zervakis, S. Konitsiotis, D. D. Koutsouris, and D. I. Fotiadis, "A long short-term memory deep learning network for the prediction of epileptic seizures using EEG signals," *Computers in biology and medicine*, vol. 99, pp. 24–37, 2018. [Online]. Available: <https://api.semanticscholar.org/CorpusID:206917364>
- [21] C. Li, X. Huang, R. Song, R. Qian, X. Liu, and X. Chen, "EEG-based seizure prediction via transformer guided CNN," *Measurement*, 2022. [Online]. Available: <https://api.semanticscholar.org/CorpusID:252347998>
- [22] J. Yan, J. Li, H. Xu, Y. Yu, and T. Xu, "Seizure prediction based on transformer using scalp electroencephalogram," *Applied Sciences*, 2022. [Online]. Available: <https://api.semanticscholar.org/CorpusID:248329925>
- [23] S. M. Usman, S. Khalid, and S. Bashir, "A deep learning based ensemble learning method for epileptic seizure prediction," *Computers in biology and medicine*, vol. 136, p. 104710, 2021. [Online]. Available: <https://api.semanticscholar.org/CorpusID:236952120>
- [24] F. Lopes, M. F. Pinto, A. Dourado, A. Schulze-Bonhage, M. Dümpelmann, and C. A. Teixeira, "Addressing data limitations in seizure prediction through transfer learning," *Scientific Reports*, vol. 14, 2024. [Online]. Available: <https://api.semanticscholar.org/CorpusID:270616596>
- [25] R. Jana and I. Mukherjee, "Deep learning based efficient epileptic seizure prediction with EEG channel optimization," *Biomedical Signal Processing and Control*, vol. 68, p. 102767, 5 2021. [Online]. Available: <https://doi.org/10.1016/j.bspc.2021.102767>
- [26] Z. Deng, C. Li, R. Song, X. Liu, R. Qian, and X. Chen, "EEG-based seizure prediction via hybrid vision transformer and data uncertainty learning," *Eng. Appl. Artif. Intell.*, vol. 123, p. 106401, 2023. [Online]. Available: <https://api.semanticscholar.org/CorpusID:258798430>
- [27] M. F. Pinto, T. Coelho, A. Leal, F. Lopes, A. Dourado, P. Martins, and C. A. Teixeira, "Interpretable EEG seizure prediction using a multiobjective evolutionary algorithm," *Scientific Reports*, vol. 12, 2022. [Online]. Available: <https://api.semanticscholar.org/CorpusID:247474253>
- [28] K. Rasheed, A. Qayyum, J. Qadir, S. Sivathamboo, P. Kwan, L. Kuhlmann, T. O'Brien, and A. Razi, "Machine Learning for Predicting Epileptic Seizures Using EEG Signals: A review," *IEEE Reviews in Biomedical Engineering*, vol. 14, pp. 139–155, 7 2020. [Online]. Available: <https://doi.org/10.1109/rbme.2020.3008792>
- [29] N. Stevenson, K. Tapani, L. Lauronen, and S. Vanhatalo, "A dataset of

- neonatal EEG recordings with seizure annotations,” <https://doi.org/10.5281/zenodo.4940267>, 2018.
- [30] D. S. Udayantha, K. Weerasinghe, N. Wickramasinghe, A. Abeyratne, K. Wickremasinghe, J. Wanigasinghe, A. D. Silva, and C. U. S. Edussooriya, “Using explainable ai for EEG-based reduced montage neonatal seizure detection,” 2024. [Online]. Available: <https://arxiv.org/abs/2406.16908>
- [31] I. B. Slimen, L. Boubchir, and H. Seddik, “Epileptic seizure prediction based on EEG spikes detection of ictal-preictal states,” *Journal of biomedical research*, vol. 34, no. 3, p. 162, 2020.
- [32] D. Wu, J. Yang, and M. Sawan, “Bridging the gap between patient-specific and patient-independent seizure prediction via knowledge distillation,” 2022. [Online]. Available: <https://pubmed.ncbi.nlm.nih.gov/35617933/>
- [33] J. Hwang, M. Hira, C. Chen, X. Zhang, Z. Ni, G. Sun, P. Ma, R. Huang, V. Pratap, Y. Zhang, A. Kumar, C.-Y. Yu, C. Zhu, C. Liu, J. Kahn, M. Ravanelli, P. Sun, S. Watanabe, Y. Shi, and Y. Tao, “TorchAudio 2.1: Advancing speech recognition, Self-Supervised Learning, and Audio Processing components for PyTorch,” Dec. 2023. [Online]. Available: <https://doi.org/10.1109/asru57964.2023.10389648>
- [34] Y.-Y. Yang, M. Hira, Z. Ni, A. Chourdia, A. Astafurov, C. Chen, C.-F. Yeh, C. Puhersch, D. Pollack, D. Genzel, D. Greenberg, E. Z. Yang, J. Lian, J. Mahadeokar, J. Hwang, J. Chen, P. Goldsborough, P. Roy, S. Narenthiran, S. Watanabe, S. Chintala, V. Quenneville-Bélair, and Y. Shi, “Torchaudio: Building blocks for audio and speech processing,” *arXiv preprint arXiv:2110.15018*, 2021.
- [35] J. Hu, L. Shen, S. Albanie, G. Sun, and E. Wu, “Squeeze-and-Excitation networks,” *IEEE Transactions on Pattern Analysis and Machine Intelligence*, vol. 42, no. 8, pp. 2011–2023, 5 2019. [Online]. Available: <https://doi.org/10.1109/tpami.2019.2913372>
- [36] S. M. Lundberg and S.-I. Lee, “A unified approach to interpreting model predictions,” in *Proceedings of the 31st International Conference on Neural Information Processing Systems*, ser. NIPS’17. Red Hook, NY, USA: Curran Associates Inc., 2017, p. 4768–4777.